DOI: 10.1002/chem.200802238

Identification of a Highly Efficient Alkylated Pincer Thioimido–Palladium(II) Complex as the Active Catalyst in Negishi Coupling

Jing Liu,[a, b] Haibo Wang,[a] Heng Zhang,[a] Xiaojun Wu,[a] Hua Zhang,[a] Yi Deng,[a] Zhen Yang,*[b] and Aiwen Lei*[a]

Abstract: The induction period of Negishi coupling catalyzed by pincer thioamide–palladium complex **1** was investigated. A heterogeneous mechanism was excluded by kinetic studies and comparison with Negishi coupling reactions promoted by $Pd(OAc)_2/Bu_4NBr$ (a palladium–nanoparticle system). Tetramer **2** was isolated from the reaction of **1** and organozinc reagents. Dissociation of complex **2** by PPh_3 was achieved, and the structure of resultant complex **8** was confirmed by X-ray diffraction analysis. A novel alkylated pincer thioimido–Pd^{II} complex, **7**, generated from catalyst precursor **1** and basic organometallic reagents (RM), was observed by in situ IR, ^1H NMR, and ^{13}C NMR spectroscopy for the first time. The reaction of **7** with methyl 2-iodobenzoate afforded 74% of the cross-coupled product, methyl 2-methylbenzoate, together with 60% of Pd^{II} complex **2**. Furthermore, the catalyst, as an electron-rich Pd^{II} species, efficiently promoted the Negishi coupling of aryl iodides and alkylzinc reagents without an induction period, even at low temperatures (0 °C or −20 °C). To evaluate the influence of the catalyst structure upon the induction period, complex **9** was prepared, in which the *n*Bu groups of **1** were displaced by more bulky 1,3,5-trimethylphenyl groups. Trimer **10** was isolated from the reaction of complex **9** and basic organometallic reagents such as CyZnCl or CyMgCl (Cy: cyclohexyl); this is consistent with the result obtained with complex **1**. The rate in the induction period of the model reaction catalyzed by **9** was faster than that with **1**. Plausible catalytic cycles for the reaction, based upon the experimental results, are discussed.

Keywords: ate complexes · coupling reactions · homogeneous catalysis · palladium · reaction mechanisms

Introduction

Palladium is among the most common transition-metal catalysts in coupling reactions today,[1,2] and a majority of Pd-catalyzed reactions have been well established or accepted as initiating from Pd^0 species. On the other hand, Pd^{II} complexes, more electron deficient yet more stable than the corresponding Pd^0 complexes, have the potential to be active catalysts as well and might offer new opportunities in both mechanistic studies and application aspects.[3–11] For example, an active Pd^{II} complex might initiate a Pd^{II}–Pd^{IV} catalytic cycle, which could address some unsolved challenges, such as the deleterious β-hydride elimination in C_{sp^3}-involved carbon–carbon bond-formation reactions,[12–17] because the reductive elimination of Pd^{IV} species has been reported to be facile due to the electron deficiency of the Pd^{IV} center.[18–20]

Theoretically, if there were enough and appropriate electron-donating surrounding ligands, the reaction of aryl halides and Pd^{II} species might be realized. Amid the palladium catalysts utilized in cross-coupling reactions so far, palladium pincer complexes, which have mainly been employed in Heck and Suzuki processes, have been proposed to involve Pd^{IV} intermediacy in some cases.[10,11] However, to date, convincing evidence is still required. Proximal thiolate ligands are known to stabilize high-valency Fe^{IV}–heme cation radicals through electron donation in biologically significant metalloenzymatic oxygenase systems.[21–25] In stoichiometric

[a] Dr. J. Liu, H. Wang, Dr. H. Zhang, X. Wu, H. Zhang, Y. Deng, Prof. A. Lei
College of Chemistry and Molecular Sciences
Wuhan University
Wuhan, Hubei, 430072 (China)
Fax: (+86) 27-6875-4067
E-mail: aiwenlei@whu.edu.cn

[b] Dr. J. Liu, Prof. Z. Yang
College of Chemistry and Molecular Engineering
Peking University
Beijing 100871 (China)
Fax: (+86) 10-6275-9105
E-mail: zyang@pku.edu.cn

Supporting information for this article is available on the WWW under http://dx.doi.org/10.1002/chem.200802238.

studies, Bennett et al. isolated a Pd^{IV} complex stabilized by a tridentate thioether ligand together with alkyl ligands, which provided further evidence of the stabilizing ability of sulfur-type ligands towards the electron-deficient Pd^{IV} center.[26] These characteristics inspired us to design and synthesize a pincer thioamide–palladium complex, **1**,[27,28] the two NH groups of which were crucial because they could be deprotonated by organozinc reagents to give the thioimido complex **2** (Scheme 1).[29,30] The thioimido ligand provided

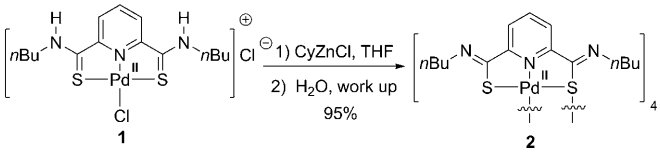

Scheme 1. Pincer thioamide–palladium complex **1** and pincer thioimido–palladium complex **2**. THF: tetrahydrofuran.

one neutral nitrogen atom, one neutral sulfur atom and two sulfur anions as electron donors for the Pd^{II} center and prevented reduction to Pd^0 species by the organozinc reagents. The catalytic capabilities of the two sulfur-containing palladium species **1** and **2** were explored in Negishi reactions involving primary and secondary alkylzinc reagents; the reactions occurred readily under mild conditions, substrates with β-hydrogen atoms were tolerated, and the catalysis was performed with unusually high efficiency.[31] Herein, we describe our mechanistic studies of sulfur-containing complex **1** in the Negishi reaction, which revealed base-induced formation of an alkylated Pd^{II} complex, and the subsequent reaction with aryl iodides.

Results and Discussion

Testing of the kinetic behavior of the Negishi coupling catalyzed by complex 1: To test the catalytic behavior of complex **1**, the coupling between ethyl 2-iodobenzoate (**3**) and cyclohexylzinc chloride (**4**) was chosen as the model reaction, with [**3**] = 0.29 M, [**4**] = 0.65 M, and [**1**] = 1.6 mM. Although complex **1** could hardly be reduced to a Pd^0 species by **4**, it promoted the reaction effectively. The reaction catalyzed by **1** was completed within 5 min with 97% yield (as measured by GC analysis) at room temperature after a short induction period (5 min), and it also progressed smoothly at 0°C after a long induction period (≈60 min), with 95% yield (Figure 1 A and B).[32]

Exclusion of a heterogeneous mechanism in the catalytic system of complex 1: The existence of induction periods and sigmoidal-shaped kinetic profiles in the catalytic system of a pincer palladium complex pointed to the possibility of the formation of palladium nanoparticles (PdNPs) as the true catalytic species. For comparison, Negishi couplings promoted by ligand-free $Pd(OAc)_2/Bu_4NBr$ were examined.[33–42]

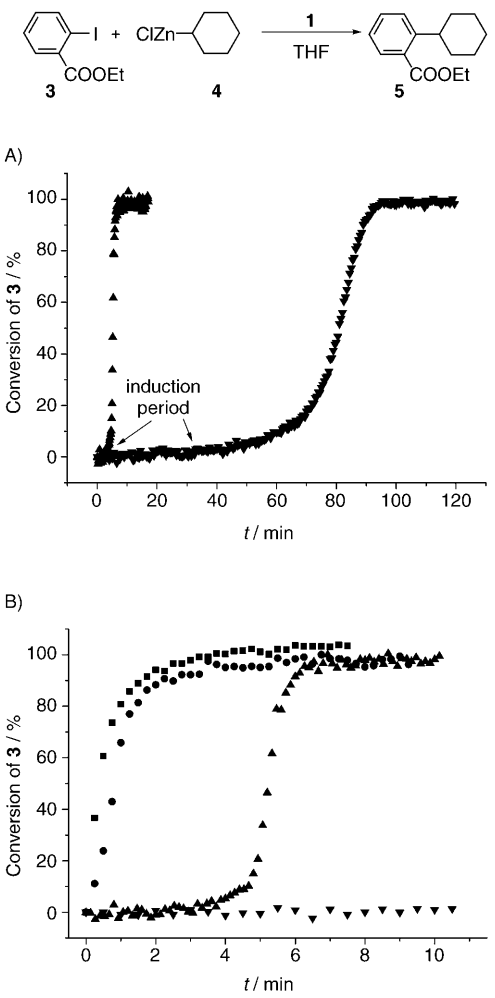

Figure 1. Conversion of ethyl 2-iodobenzoate (**3**) into cross-coupled product **5**, as monitored by the ReactIR system (see the Experimental Section), with [**3**] = 0.29 M, [**4**] = 0.65 M, and [Pd] = 1.6 mM (▲: [**1**] = 1.6 mM, 25°C; ▼: [**1**] = 1.6 mM, 0°C; ■: $[Pd(OAc)_2]$ = 1.6 mM, $[Bu_4NBr]$ = 0.29 M, 25°C; ●: $Pd(OAc)_2]$ = 1.6 mM, $[Bu_4NBr]$ = 0.29 M, 0°C).

The reaction was finished within 2 min without an induction period at 25°C, and the kinetic plot was similar at 0°C (Figure 1 B). The induction periods of these two reactions were not as sensitive to temperature as those involving **1** as the catalyst precursor (Figure 1).

Ligand inhibition experiments have been proven to be an efficient method to clarify whether a reaction was catalyzed by a homogenous catalyst or NPs.[34,43] Figure 2 illustrates our experimental results. When PPh_3 (0.7 equiv relative to Pd) was added to the mixture of **3**, **4**, and catalyst **1** (2 mol%), the reaction was completed within 3 min with 96% yield (Figure 2). However, PPh_3 (0.5 equiv relative to Pd) significantly inhibited the reaction when $Pd(OAc)_2$ (2 mol%) was used as the catalyst precursor. Within 30 min, 30% of **3** was converted, of which only 14% was converted into the cross-coupled product **5** (as detected by GC analysis); 16% of the dehalogenated product, ethyl benzoate, was formed.[44] Comparison of the two reactions suggested that the active catalyst formed from **1** was not a PdNP system.

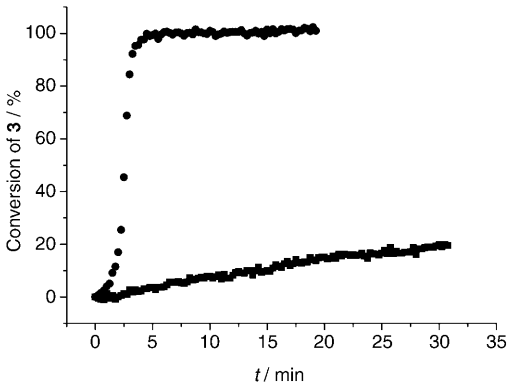

Figure 2. Quantitative poisoning experiments: conversion of ethyl 2-iodobenzoate (**3**), as monitored by the ReactIR system (see the Experimental Section), with [**3**] = 0.29 M and [**4**] = 0.65 M (●: [**1**] = 6.4 mM, [PPh_3] = 4.5 mM, 25 °C; ■: [$Pd(OAc)_2$] = 6.4 mM, [Bu_4NBr] = 0.29 M, [PPh_3] = 3.2 mM, 25 °C).

Furthermore, kinetic measurements were conducted for the reaction of **3** with excess **4** in the presence of different amounts of catalyst **1** in THF at 25 °C, with [**3**] = 0.29 M, [**4**] = 0.65 M, and [**1**] = 0.16–0.98 mM. A linear plot of the observed rate (k_{obs}) versus [**1**] showed the reaction to be first order with respect to catalyst **1** (see Figure 4 in the Supporting Information). It has been reported that the reaction rate is not first order with respect to the concentration of the catalyst when NPs are the true catalytic species.[42,45–49] Therefore, these data further supported the conclusion that **1** was homogenous rather than heterogeneous in this catalytic system.

Proposal for the induction period: formation of an electron-rich ate complex as the active catalyst: To probe the induction period, we investigated stoichiometric reactions of complex **1** and the two reactants **3** and **4**. No obvious reaction was observed when **1** and **3** were mixed together in THF at between 0 °C and 60 °C. However, when zinc reagent **4** (10 equiv relative to **1**) was added in to the system, the reaction progressed smoothly and 74% of the cross-coupled product **5** was obtained; this indicated the involvement of cyclohexylzinc chloride (**4**) in the active-catalyst formation process.

As mentioned above, direct reaction of **1** with **4** gave the more electron-rich Pd^{II} complex **2** instead of reducing **1** to the Pd^0 species (Scheme 1). Yet a long induction period existed when complex **2** was used as the catalyst precursor (see Figure 7 in the Supporting Information), and the stoichiometric reaction of **2** and **3** could only occur in the presence of excess **4**. Therefore, a further reaction of **2** with cyclohexylzinc chloride (**4**) was necessary to generate the active catalyst.

By comparing the structures of complexes **1** and **2**, and on the basis of the experiments above, we could reasonably speculate that the alkylzinc reagent should first deprotonate the NH groups of **1** to generate **6**, as shown in Scheme 2. Aggregation of **6** resulted in the formation of **2**. In the presence of excess alkylzinc halide, complex **6** might be further alkylated to yield complex **7**, which is an anionic complex with two S anions, one N atom, and one C_{sp^3} anion capable of donating electrons towards the palladium center; hence, **7** is possibly electronically rich enough to react with aryl iodides.[51] Consumption of **6** by alkylation to form **7** could draw the equilibrium from **2** toward **6**. Yet the alkylation of **6** by the organozinc reagent was a minor process (see Figure 4 below), probably due to the low reactivity and nucleophilicity of the zinc reagents, and aryl iodide was required to react with **7** to enable the alkylation to proceed. Anionic Pd^0 adducts as precursors for oxidative addition in catalytic systems have been proposed,[52–54] but corresponding Pd^{II} species have rarely been reported.[55–57]

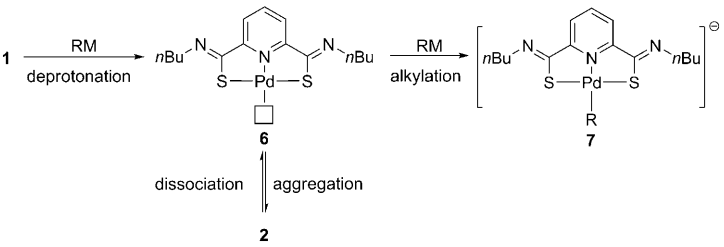

Scheme 2. Proposal for ate complex **7** as the active catalyst.[50]

Identification of ate complex 7: To explore the feasibility of the dissociation process (Scheme 2), **2** was treated with PPh_3 (1 equiv relative to Pd).[56,57] The tetrameric structure was dissociated, and complex **8**, the structure of which was con-

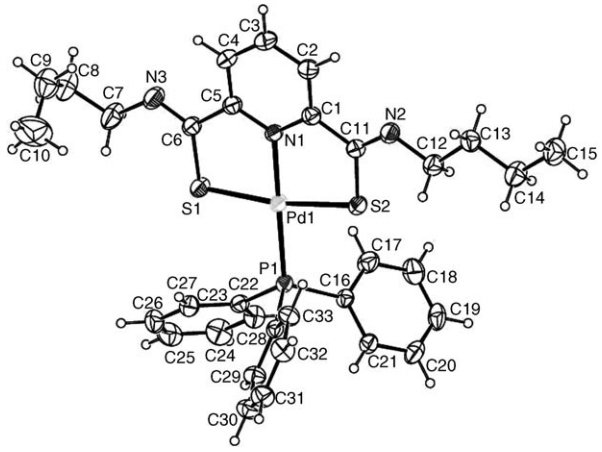

Figure 3. Single-crystal structure of complex **8**.

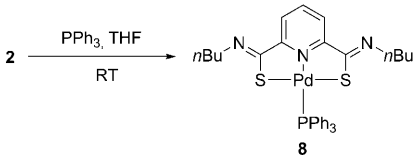

Scheme 3. Dissociation of **2** by PPh_3.

firmed by X-ray diffraction analysis (Figure 3), was obtained in quantitative yield (Scheme 3).[58]

In situ monitoring of the reaction of **1** and **4** (10 equiv) revealed the formation of only one new component in 1 min (Figure 4A) with absorbances at $\tilde{\nu}=1606$, 1571, and 1562 cm^{-1} (Figure 4B), which tallied with those for complex **2** (Figure 5). Thus, the intermediate was assigned as **6** or **2** because both compounds possess similar functional groups for IR absorbance. The results indicated that the deprotonation was a fast process and little or no alkylation to produce complex **7** occurred in this system.

^{13}C NMR detection for the reaction of tetramer **2** with MeZnCl (2 equiv) revealed that **2** remained unchanged, which further confirmed the above results (see Figure 10 in the Supporting Information).[59]

Grignard reagents are usually more electronegative and reactive than the corresponding zinc reagents, so we envisaged that the formation of **7** would be easier with Grignard reagents. Hence, the stoichiometric reaction of complex **1** and CyMgCl was monitored by in situ IR spectroscopy, and two components were observed (**A** and **B** in Figure 6A).

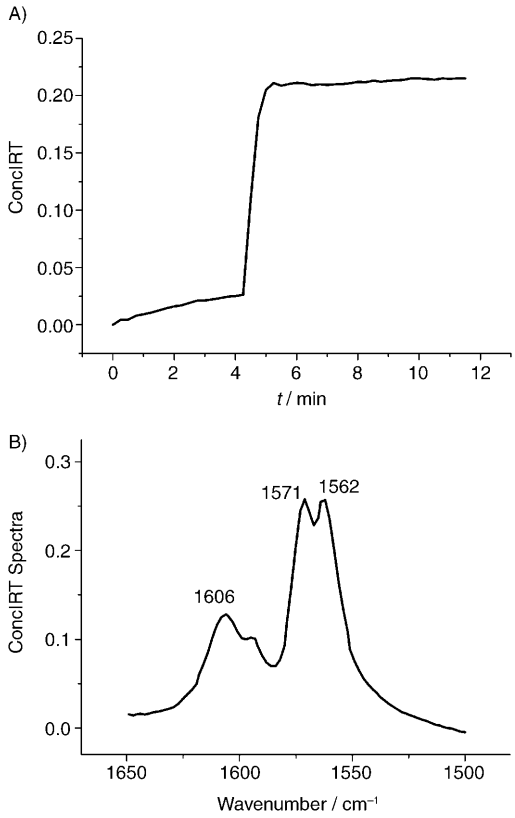

Figure 4. Reaction of **1** (24.3 mg, 0.05 mmol) with **4** (0.8 mL, 0.5 mmol) in THF at 25 °C, as monitored by the ReactIR system (see the Experimental Section). A) The absorbance of the newly formed component versus time; B) the ConcIRT spectrum of the newly formed component.

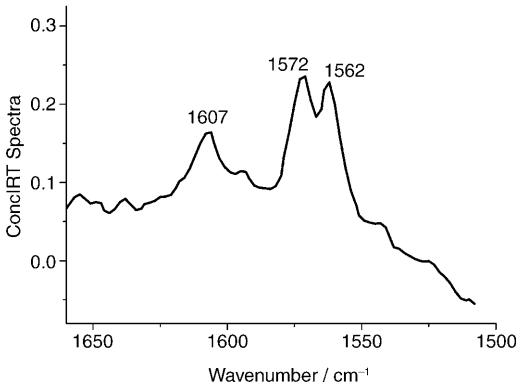

Figure 5. The ConcIRT spectrum of tetramer **2**.

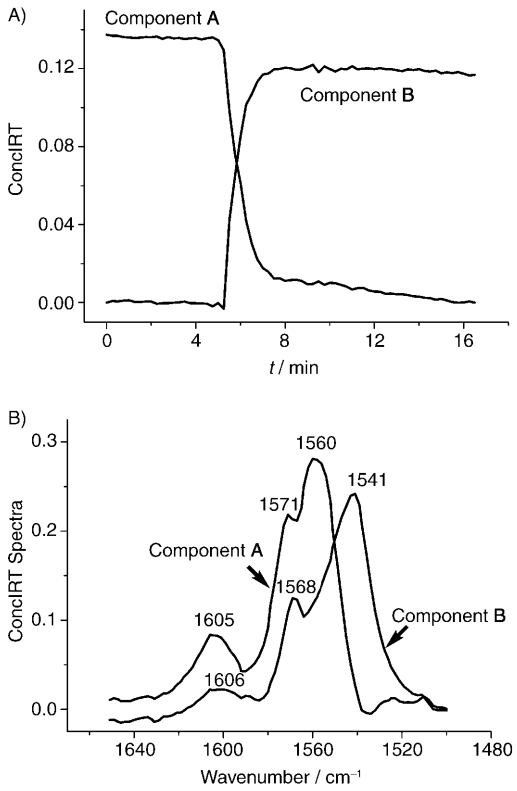

Figure 6. Reaction of **1** (24.3 mg, 0.05 mmol) with CyMgCl (0.2 mL, 0.28 mmol) in THF, as monitored by the ReactIR system (see the Experimental Section). A) The concentration of components **A** and **B** versus time; B) the ConcIRT spectra of components **A** and **B**.

The ConcIRT spectra of component **A** (Figure 6B) tallied with the IR spectrum in Figure 4B, which suggested that the kinetic profile of component **A** (Figure 6A) represented a change of complex **6** or **2**. The spectrum of the newly formed component **B** (Figure 6B) shifted to lower wavenumbers than that of **A** (1541 cm^{-1} instead of 1560 cm^{-1}). This phenomenon was rationalized as arising from the electron-density increase of the palladium center upon alkylation to form **7**. When CyMgCl was added to the mixture of complex **1** and CyZnCl, the spectrum of the newly generated complex was the same as that of component **B** (see Figure 9 in the Supporting Information).

To validate the aforementioned assumption, **1** was treated with MeMgCl (5 equiv) in THF and monitored by NMR spectroscopy. ^{13}C NMR spectroscopy revealed the appearance of a peak at $\delta = -21.7$ ppm and supported the existence of a Pd–Me bond (see the Supporting Information). Importantly, the reaction between **1** and a smaller amount of MeMgCl (3.2 equiv) afforded a similar ^{13}C NMR spectra with a peak at $\delta = -21.7$ ppm (see Figure 8 A and the Supporting Information). In the ^{1}H NMR spectrum (Figure 7),

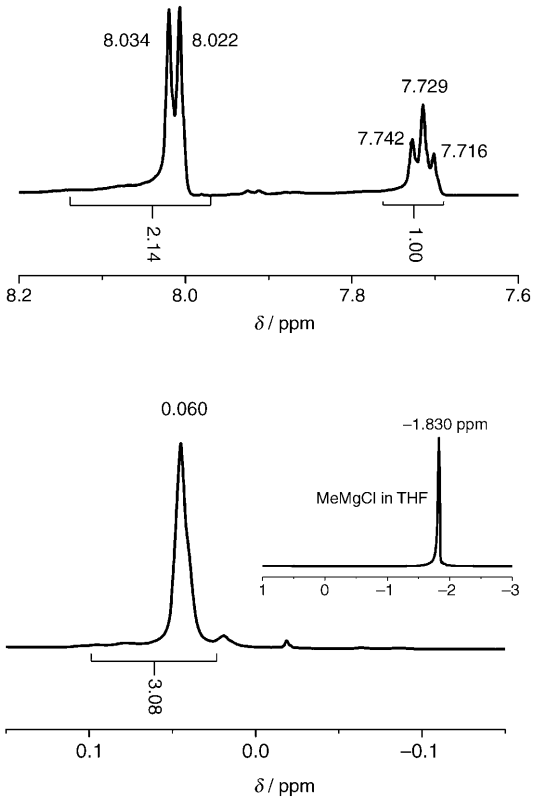

Figure 7. Selected regions of the ^{1}H NMR spectrum (600 MHz) following the reaction of **1** with MeMgCl (3.2 equiv) in THF.

the peak corresponding to 3H atoms at $\delta = 0.060$ ppm was assigned to the methyl group attached to the palladium center. In the lowfield region, a duplet peak corresponding to 2H atoms at $\delta = 8.028$ ppm and a triplet peak equivalent to 1H atom at $\delta = 7.729$ ppm indicated that the resultant complex was symmetrical. All of this information was consistent with the proposed structure of the alkylated complex **7** (R: Me) shown in Scheme 2.

Testing of the activity of ate complex 7: The reaction mixture of complex **1** and MeMgCl (3.2 equiv) was treated with methyl 2-iodobenzoate (10 equiv) at room temperature and monitored by ^{13}C NMR spectroscopy (Figure 8). The peak at $\delta = -21.7$ ppm disappeared as expected; 74% of methyl 2-methylbenzoate, the cross-coupled product, was obtained (as determined by ^{1}H NMR spectroscopy), together with 60% of the Pd^{II} complex tetramer **2** (Scheme 4). This proved that complex **7** was active toward the aryl iodide.

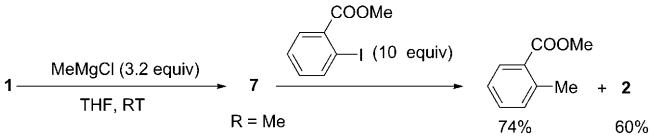

Scheme 4. Stoichiometric reaction of complex **7**.

Addition of 2,2,6,6-tetramethyl-1-piperidinoxyl (TEMPO; 1 equiv relative to Pd) to the reaction mixture of **1** and MeMgCl (3.2 equiv) before addition of the aryl iodide had little influence on the reaction yield. Thus, radical pathways for the reaction of complex **7** with methyl 2-iodobenzoate were disfavored.[60]

To test the catalytic activity of complex **7**, **1** (0.5 mol%) was treated with CyMgBr (2.5 mol%) at 0°C for 2 min; this was followed by immediate addition of CyZnCl (**4**) and aryl iodide **3**. To our great pleasure, no induction period was observed, just as expected, and the reaction took only 8 min to reach 100% conversion (98% yield of the cross-coupled product **5** as monitored by GC analysis; Figure 9). It is noteworthy that the reaction of **3** and **4** also occurred smoothly at −20°C after catalyst **1** had been pretreated with CyMgCl at −20°C and no induction period existed under these conditions either (Figure 9).

Evaluation of the influence of the catalyst structure upon the induction period: To explore the influence of the catalyst structure upon the induction period, we prepared complex **9** in which the *n*Bu groups were displaced by more bulky 1,3,5-trimethylphenyl groups (Scheme 5). A trimer was isolated from the reaction of complex **9** and basic organometallic reagents, such as CyZnCl or CyMgCl

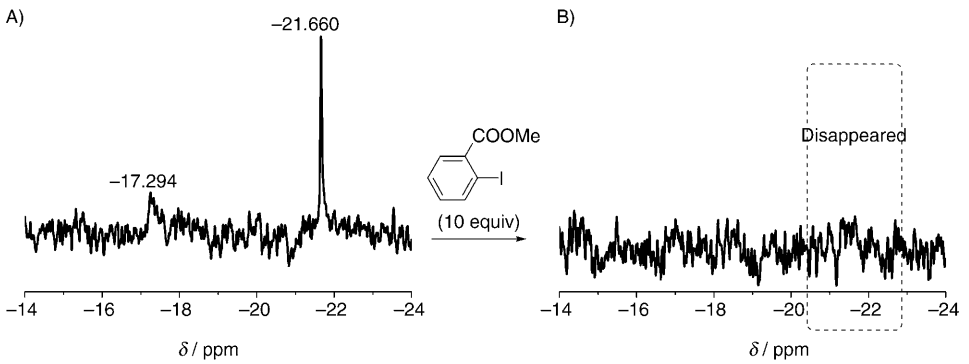

Figure 8. A) Selected region of the ^{13}C NMR spectrum following the reaction of **1** with MeMgCl (3.2 equiv) in THF. B) Selected region of ^{13}C NMR spectrum of the mixture in **I** after addition of methyl 2-iodobenzoate (10 equiv).

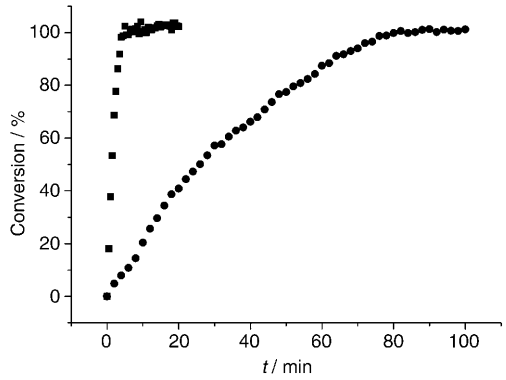

Figure 9. Kinetic profiles of the reaction of **3** and **4** at 0°C (■) and −20°C (●) catalyzed by complex **7** (R: Cy).

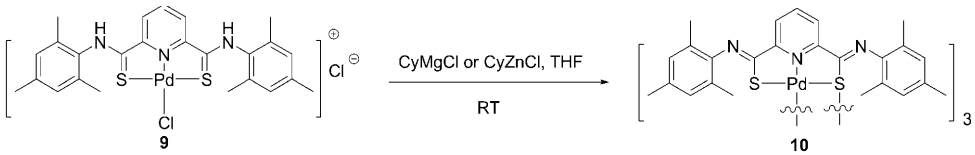

Scheme 5. Deprotonation of complex **9**.

(Scheme 5 and Figure 10), which is consistent with the result for complex **1** (Scheme 1). The lengths of the Pd–S bonds broken in the dissociation process were similar (2.314 Å for **2** versus 2.317 Å for **10**), but the S–Pd–S angles were quite different. The angle in **2** was 112.21°, whereas that in **10** was 98.9°, which indicates that the ring strain of the latter was greater than that of the former. Also, π–π stacking observed in complex **2** could decelerate the dissociation of the complex by a stabilization effect, whereas the greater steric hindrance around the Pd–S ring in **10** might accelerate the dissociation process.[61] Monitoring the model reaction catalyzed by **9** at 15°C revealed a kinetic plot different from that for the reaction catalyzed by complex **1** (Figure 11). The rate in the induction period of the former reaction was faster than that of the latter, whereas the rate in the period afterwards was slower than that of the latter. Theoretically, the steric hindrance of the 1,3,5-trimethylphenyl groups would accelerate the dissociation process of the trimer (see above) and decelerate the alkylation process to form the ate complex. Thus, the rate increase in the induction period was probably due to the acceleration of the dissociation process, and the rate decrease after the induction period might result from the lower reactivity of the ate complex because of the increased steric hindrance and the decreased electron density of the Pd^{II} center.

Discussion about the induction period and the subsequent steps of the Negishi coupling catalyzed by pincer thioamide–palladium or pincer thioimido–palladium complexes: In the process of investigating the reactivities of monoorganozinc and diorganozinc reagents in the Negishi coupling catalyzed by pincer thioamide–palladium or pincer thioimido–palladium

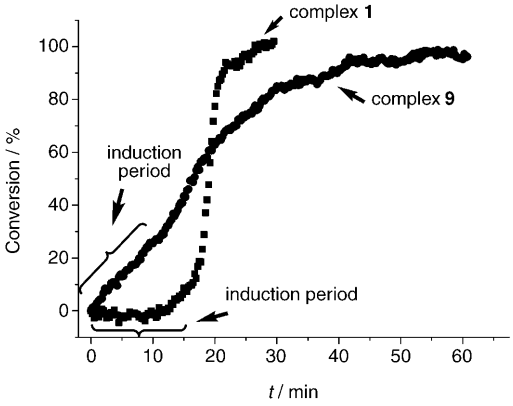

Figure 11. Conversion of ethyl 2-iodobenzoate (**3**), as monitored by the ReactIR system (see the Experimental Section), at 15°C with initial concentrations of [**3**] = 0.16 M, [**4**] = 0.39 M, and [catalyst] = 1.6 mM.

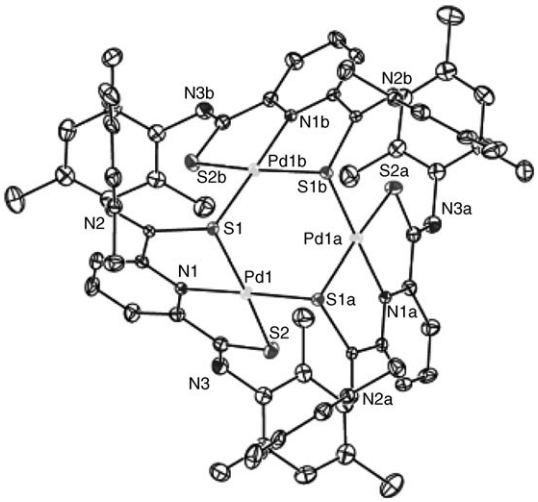

Figure 10. Single-crystal structure of complex **10**.

complexes, two plausible pathways were proposed to rationalize the differences between the two type of zinc reagents (Scheme 6).[31] Deprotonation of the catalyst precursor **I** resulted in monomer **III**. **III** was inclined to aggregate to form complex **II** and to stay out of the catalytic cycle. However, under certain conditions, **II** could dissociate to release **III**. **III** could be alkylated by organometallic reagents, such as organozinc or Grignard reagents, to afford ate complex **IV**, which was proven to be active toward aryl iodides. Reductive elimination of **V** afforded the cross-coupled product ArR and returned to complex **III** (path A). Alternatively, complex **III** might be further alkylated to produce **VI**, which upon reductive elimination would release **IV** (path B).[62]

The deprotonation process was displayed clearly by the formation of complexes **2** and **10**. Stoichiometric and cata-

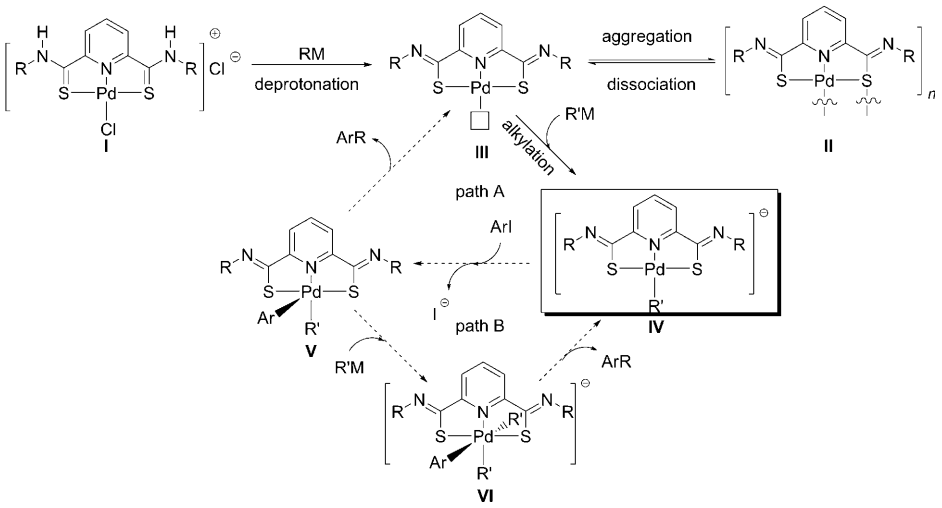

Scheme 6. Speculative mechanism for the Negishi coupling catalyzed by pincer thioamide–palladium or pincer thioimido–palladium complexes.

lytic reactions manifested that **II** was not the active catalyst and that dissociation was required to enable the complex to enter the catalytic cycle. The structure of ate complex **IV** was established by spectroscopic data. The reactivity of **IV** toward aryl iodides was proven stoichiometrically and catalytically. Radical pathways were disfavored because little influence of TEMPO was observed in the stoichiometric reaction of the ate complex with aryl iodide. Therefore, Pd intermediate **V** was proposed.

If **V** went through direct reductive elimination (path A), **III** would be regenerated and the dissociation of **II** would be responsible for the induction period. On the other hand, if **V** underwent further alkylation to produce **VI**, **IV** would be regenerated after reductive elimination and both the dissociation of **II** and the alkylation of **III** would be responsible for the induction period.

As shown above, utilization of a more reactive Grignard reagent (to affect the alkylation process) and the more hindered complex **9** (to affect the dissociation process) both influenced the induction period. Therefore, path B possibly occurs in the catalytic process. However, the participation of path A could not be excluded because the joint operation of both pathways would be consistent with the experimental results too.

Conclusion

In conclusion, a heterogeneous mechanism for the Negishi coupling catalyzed by pincer thioamide–palladium complex **1** was excluded by kinetic investigations. A novel alkylated pincer thioimido–Pd^{II} complex, **7**, generated from catalyst precursor **1** and basic metal reagents, was observed by in situ IR, ^{1}H NMR, and ^{13}C NMR spectroscopy for the first time, and it was proven to be the active catalyst by stoichiometric and catalytic reactions. The catalyst, as an electron-rich Pd^{II} species, could react with aryl iodides to afford cross-coupled products and displayed high efficiency even at −20 °C.[63] The induction period of the reaction could be influenced by both the alkylation reagents and the catalyst structures. Plausible catalytic cycles for the reaction were discussed based upon the experimental results, and further studies to clarify the subsequent mechanistic steps are ongoing in our laboratory and will be reported in due course.

Experimental Section

Toluene and THF were dried and distilled from sodium/benzophenone immediately prior to use under a nitrogen atmosphere. CH_3CN was dried over anhydrous sodium sulfate (Na_2SO_4). Analytical grade solvents and commercially available reagents were used as received, unless otherwise stated.

Glass 0.25 mm silica gel plates were employed for thin-layer chromatography (TLC). Flash-chromatography columns were packed with 200–300 mesh silica gel or neutral alumina with 200–300 mesh in petroleum (boiling point = 60–90 °C). Gradient flash chromatography was conducted by eluting with a continuous gradient from petroleum to the indicated solvent (v/v ratios are given).

^{1}H and ^{13}C NMR data were recorded with a Varian Mercury VX300 (300 MHz) or a Varian Mercury VX600 (600 MHz) spectrometer. All ^{1}H NMR chemical shifts (δ in ppm) are reported relative to the internal or external standard. Coupling constants (J) are reported in Hertz (Hz). High-resolution mass spectra (HRMS) were measured with a Waters Micromass GCT instrument, and accurate masses are reported for the molecular ion [M^+]. GC yields were recorded with a Varian GC 3900 gas chromatography instrument with an FID detector. For the ReactIR kinetic experiments, the reaction spectra were recorded by using a IC 10 apparatus from Mettler-Toledo AutoChem fitted with a diamond-tipped probe. Data manipulation was carried out by using the iC IR (version 1.05)[65] software.

Crystal diffraction intensity data were collected on a Bruker CCD 4K diffractometer with graphite-monochromatized Mo Kα radiation (λ = 0.71073 Å). Lattice determination and data collection were carried out by using SMART (version 5.625)[66] software. Data reduction and absorption corrections were performed by using SAINT (version 6.45)[67] and SADABS (version 2.03)[68] software. Structure solution and refinement were performed by using the SHELXTL (version 6.14)[69] software package.

Representative procedure for the catalytic reaction of 3 and 4 monitored by ReactIR: The spectra were acquired in 33 scans at a gain of 1 and a resolution of 2 by using the ReactIR (version 1.05) software. The reaction was carried out as follows. **1** (2.4 mg, 0.54 mol %) was added to an oven-dried three-necked reaction vessel fitted with a magnetic stirring bar. The IR probe was then inserted through an adapter into the middle neck; the other two necks were capped by rubber septums. The reaction vessel was evacuated and flushed with nitrogen 3 times, put into a 25 °C bath, and charged with cyclohexylzinc chloride (**4**; 3.0 mL THF solution, 1.95 mmol). The data collection was then started. Ethyl 2-iodobenzoate (**3**; 254 mg, 0.92 mmol) was added to initiate the reaction, and data collection was continued until the reaction was finished. Cross-coupled product **5** (ethyl 2-cyclohexylbenzoate)[64] was characterized by ^{1}H NMR and ^{13}C NMR spectroscopy: ^{1}H NMR (300 MHz, $CDCl_3$): δ = 7.71 (dd,

J=7.8, 1.2 Hz, 2H), 7.46–7.36 (m, 2H), 7.23–7.18 (m, 1H), 3.70 (q, J= 7.2 Hz, 2H), 3.32–3.25 (m, 1H), 1.89–1.74 (m, 5H), 1.45–1.37 ppm (m, 8H); ^{13}C NMR (75.4 MHz, $CDCl_3$): δ=168.53, 148.16, 131.31, 130.39, 129.58, 126.63, 125.25, 60.73, 40.15, 34.24, 26.85, 26.13, 14.17 ppm.

Synthesis of Pd complex 8: Complex **2** (41.3 mg, 0.1 mmol Pd) and PPh_3 (26.2 mg, 0.1 mmol) were added to a dry Schlenk tube under N_2. Purified THF (1 mL) was then injected, and a red solution was formed. The solution was stirred overnight and a yellow solid precipitated. The solvent was removed by rotary evaporation, and the residue was dried under vacuum for 2 h to afford product **8** as a yellow solid (68.0 mg, 99%). Recrystallization from CH_2Cl_2/hexane gave red block-shaped crystals of **8** that were suitable for X-ray diffraction: ^{1}H NMR (300 MHz, $CDCl_3$): δ= 8.11 (d, J=7.5 Hz, 2H), 7.87–7.60 (m, 7H), 7.59–7.29 (m, 9H), 3.55 (t, J=6.9 Hz, 4H), 1.77–1.64 (m, 4H), 1.52–1.36 (m, 4H), 0.94 ppm (t, J= 7.4 Hz, 6H); ^{13}C NMR (75 MHz, $CDCl_3$): δ=169.40, 159.80, 136.56, 134.50, 134.34, 131.17, 130.20, 129.49, 128.46, 128.31, 123.83, 53.05, 32.65, 20.87, 14.05 ppm; HRMS (MALDI; 2,5-dihydroxybenzoic acid): m/z calcd for $C_{33}H_{36}N_3PPdS_2$ $[M+H]^+$: 675.1123; found: 675.1121.

Formation of ate complex 7 (R: Me): **1** (24.3 mg, 0.05 mmol) was put into an NMR spectroscopy tube, and the tube was placed in a glove box. Dry THF (0.1 mL) was added to the tube, followed by dropwise addition of a THF solution of MeMgCl (80 μL, 0.25 mmol). After the reaction mixture stopped bubbling, a clear reddish-orange solution was obtained. $CDCl_3$ sealed in a capillary was put into the tube as an external standard, the tube was then capped and removed from the glove box, and the contents of the tube were characterized by ^{13}C NMR spectroscopy: ^{13}C NMR (150 MHz, THF): δ=176.94, 157.80, 134.05, 121.16, 53.36, 33.44, 21.17, 13.97, −17.204, −21.68 ppm.

Reaction of complex 7 with methyl 2-iodobenzoate: **1** (24.3 mg, 0.05 mmol) was put into an NMR spectroscopy tube, and the tube was placed in a glove box. Dry THF (0.1 mL) was added to the tube, followed by dropwise addition of a THF solution of MeMgCl (51 μL, 0.16 mmol). After the reaction mixture stopped bubbling, a clear reddish-orange solution was obtained. Methyl 2-iodobenzoate (75 μL, 0.5 mmol) was added, and the color of the solution became darker. $CDCl_3$ sealed in capillary was put into the tube as an external standard, the tube was then capped and removed from the glove box, and the contents of the tube were characterized by ^{13}C NMR spectroscopy. The peak observed at δ=−21.7 ppm for complex **7** had disappeared. The resultant solution was then transferred to a round-bottomed flask. The NMR tube was rinsed three times with CH_2Cl_2. The organic phases were combined and subjected to neutral Al_2O_3 column chromatography (2% ethyl acetate in petroleum ether to give the mixture of organic compounds, followed by 2% CH_3OH in CH_2Cl_2 to give complex **2**). The yields of the cross-coupled product methyl 2-methylbenzoate and complex **2** were determined to be 74% and 60% respectively by ^{1}H NMR spectroscopy with CH_2Br_2 as the internal standard.

The cross-coupled product methyl 2-methylbenzoate[70] obtained after further purification was characterized by ^{1}H NMR and ^{13}C NMR spectroscopy: ^{1}H NMR (600 MHz, $CDCl_3$): δ=7.90 (d, J=7.8 Hz, 1H), 7.30–7.20 (m, 2H), 3.87 (s, 3H), 2.59 ppm (s, 3H); ^{13}C NMR (150 MHz, $CDCl_3$): δ=168.0, 140.1, 131.9, 131.6, 130.5, 129.4, 125.6, 51.7, 21.7 ppm.

Acknowledgements

This work was supported by the National Natural Science Foundation of China (grant nos.: 20772093, 20502020, and 20832003), the Excellent Youth Foundation of the Hubei Scientific Committee, a postdoctoral research fund (grant no.: 203-180549), and a startup fund from Wuhan University.

[1] F. Zeng, E.-i. Negishi, *Org. Lett.* **2002**, *4*, 703–706.
[2] A. de Meijere, F. Diederich, *Metal-catalyzed cross-coupling reactions*, 2nd ed., Wiley-VCH, Weinheim, **2004**.
[3] M. Catellani, G. P. Chiusoli, C. Castagnoli, *J. Organomet. Chem.* **1991**, *407*, C30–C33.
[4] G. Bocelli, M. Catellani, S. Ghelli, *J. Organomet. Chem.* **1993**, *458*, C12–C15.
[5] M. Ohff, A. Ohff, M. E. van der Boom, D. Milstein, *J. Am. Chem. Soc.* **1997**, *80*, 11687–11688.
[6] D. Kalyani, N. R. Deprez, L. V. Desai, M. S. Sanford, *J. Am. Chem. Soc.* **2005**, *127*, 7330–7331.
[7] O. Daugulis, V. G. Zaitsev, *Angew. Chem.* **2005**, *117*, 4114–4116; *Angew. Chem. Int. Ed.* **2005**, *44*, 4046–4048.
[8] R. Giri, N. Maugel, J.-J. Li, D.-H. Wang, S. P. Breazzano, L. B. Saunders, J.-Q. Yu, *J. Am. Chem. Soc.* **2007**, *129*, 3510–3511.
[9] R. Giri, J. Liang, J.-G. Lei, J.-J. Li, D.-H. Wang, X. Chen, I. C. Naggar, C. Guo, B. M. Foxman, J.-Q. Yu, *Angew. Chem.* **2005**, *117*, 7586–7590; *Angew. Chem. Int. Ed.* **2005**, *44*, 7420–7424.
[10] M. E. van der Boom, D. Milstein, *Chem. Rev.* **2003**, *103*, 1759–1792.
[11] M. Albrecht, G. van Koten, *Angew. Chem.* **2001**, *113*, 3866–3898; *Angew. Chem. Int. Ed.* **2001**, *40*, 3750–3781.
[12] J. F. Hartwig, *Inorg. Chem.* **2007**, *46*, 1936–1947.
[13] T.-Y. Luh, M.-k. Leung, K.-T. Wong, *Chem. Rev.* **2000**, *100*, 3187–3204.
[14] F. Ozawa, T. Ito, Y. Nakamura, A. Yamamoto, *Bull. Chem. Soc. Jpn.* **1981**, *54*, 1868–1880.
[15] F. O. Arp, G. C. Fu, *J. Am. Chem. Soc.* **2005**, *127*, 10482–10483.
[16] M. R. Netherton, G. C. Fu, *Adv. Synth. Catal.* **2004**, *346*, 1525–1532.
[17] J. Zhou, G. C. Fu, *J. Am. Chem. Soc.* **2003**, *125*, 14726–14727.
[18] C. Duecker-Benfer, R. van Eldik, A. J. Canty, *Organometallics* **1994**, *13*, 2412–2414.
[19] B. A. Markies, A. J. Canty, J. Boersma, G. van Koten, *Organometallics* **1994**, *13*, 2053–2058.
[20] A. Moravskiy, J. K. Stille, *J. Am. Chem. Soc.* **1981**, *103*, 4182–4186.
[21] *Cytochrome P450: Structure, Mechanism, and Biochemistry*, 2nd ed. (Ed.: P. R. Ortiz de Montellano), Springer, Heidelberg, **1995**.
[22] J. H. Dawson, *Science* **1988**, *240*, 433–439.
[23] T. Higuchi, S. Uzu, M. Hirobe, *J. Am. Chem. Soc.* **1990**, *112*, 7051–7053.
[24] T. Higuchi, K. Shimada, N. Maruyama, M. Hirobe, *J. Am. Chem. Soc.* **1993**, *115*, 7551–7552.
[25] H.-A. Wagenknecht, W.-D. Woggon, *Angew. Chem.* **1997**, *109*, 404–407; *Angew. Chem. Int. Ed. Engl.* **1997**, *36*, 390–392.
[26] M. A. Bennett, A. J. Canty, J. K. Felixberger, L. M. Rendina, C. Sunderland, A. C. Willis, *Inorg. Chem.* **1993**, *32*, 1951–1958.
[27] R. A. Begum, D. Powell, K. Bowman-James, *Inorg. Chem.* **2006**, *45*, 964–966.
[28] M. A. Hossain, S. Lucarini, D. Powell, K. Bowman-James, *Inorg. Chem.* **2004**, *43*, 7275–7277.
[29] The yield of **2** was improved by optimization of the workup procedures of the reaction; see the Supporting Information.
[30] The deprotonation process was solvent dependent and was much slower in diethyl ether. The difference was speculated to arise from the solvent-dependent Schlenk equilibrium of the alkylzinc reagents; see the Supporting Information for a detailed discussion.
[31] H. Wang, J. Liu, Y. Deng, T. Min, G. Yu, X. Wu, Z. Yang, A. Lei, *Chem. Eur. J.* **2009**, *15*, 1499-1507.
[32] The model reaction in diethyl ether was much slower than that in THF and the induction period was much longer, probably because of the solvent-dependent Schlenk equilibrium of the alkylzinc reagents. See reference [30] and the Supporting Information.
[33] A. H. M. De Vries, F. J. Parlevliet, L. Schmieder-Van De Vondervoort, J. H. M. Mommers, H. J. W. Henderickx, M. A. M. Walet, J. G. De Vries, *Adv. Synth. Catal.* **2002**, *344*, 996–1002.
[34] J. A. Widegren, R. G. Finke, *Mol. Catal. A* **2003**, *198*, 317–341.
[35] A. Alimardanov, L. Schmieder-van de Vondervoort, A. H. M. de Vries, J. G. de Vries, *Adv. Synth. Catal.* **2004**, *346*, 1812–1817.
[36] M. R. Eberhard, *Org. Lett.* **2004**, *6*, 2125–2128.
[37] K. Yu, W. Sommer, M. Weck, C. W. Jones, *J. Catal.* **2004**, *226*, 101–110.
[38] D. E. Bergbreiter, P. L. Osburn, J. D. Frels, *Adv. Synth. Catal.* **2005**, *347*, 172–184.

[39] S. J. Broadwater, D. T. McQuade, *J. Org. Chem.* **2006**, *71*, 2131–2134.
[40] N. T. S. Phan, M. Van Der Sluys, C. W. Jones, *Adv. Synth. Catal.* **2006**, *348*, 609–679.
[41] D. Astruc, *Inorg. Chem.* **2007**, *46*, 1884–1894.
[42] M. T. Reetz, J. G. de Vries, *Chem. Commun.* **2004**, 1559–1563.
[43] Y. Lin, R. G. Finke, *Inorg. Chem.* **1994**, *33*, 4891–4910.
[44] Hg drop tests did not succeed in either reaction, probably because the amalgamation was much slower than the reaction rate under the above mild conditions, which are different from the usual high-temperature conditions for pincer palladium catalytic systems. Also, the excess mercury in the reaction system might cause decomposition of the zinc reagent or interact with the ligand as a sulfurphilic metal, which would destroy the catalyst.
[45] G. P. F. Van Strijdonck, M. D. K. Boele, P. C. J. Kamer, J. G. De Vries, P. W. N. M. Van Leeuwen, *Eur. J. Inorg. Chem.* **1999**, 1073–1076.
[46] A. H. M. de Vries, J. M. C. A. Mulders, J. H. M. Mommers, H. J. W. Henderickx, J. G. de Vries, *Org. Lett.* **2003**, *5*, 3285–3288.
[47] I. J. S. Fairlamb, S. Grant, P. McCormack, J. Whittall, *Dalton Trans.* **2007**, 859–865.
[48] I. J. S. Fairlamb, R. J. K. Taylor, J. L. Serrano, G. Sanchez, *New J. Chem.* **2006**, *30*, 1695–1704.
[49] J. G. De Vries, *Dalton Trans.* **2006**, 421–429.
[50] The vacant site of **6** might be coordinated by solvent THF.
[51] Low conversion (<5%) was observed within 90 min at 0 °C with the pincer Pd^0 complex generated in situ from Pd(*trans,trans*-dibenzylideneacetone)$_2$ and the pincer ligand.
[52] C. Amatore, A. Jutand, *Acc. Chem. Res.* **2000**, *33*, 314–321.
[53] L. M. Alcazar-Roman, J. F. Hartwig, *J. Am. Chem. Soc.* **2001**, *123*, 12905–12906.
[54] E. Poverenov, M. Gandelman, L. J. W. Shimon, H. Rozenberg, Y. Ben-David, D. Milstein, *Chem. Eur. J.* **2004**, *10*, 4673–4684.
[55] B. L. Shaw, *Chem. Commun.* **1998**, 1361–1362.
[56] D. Sellmann, C. Allmann, F. Heinemann, F. Knoch, J. Sutter, *J. Organomet. Chem.* **1997**, *541*, 291–305.
[57] D. Sellmann, F. Geipel, F. W. Heinemann, *Eur. J. Inorg. Chem.* **2000**, 271–279.
[58] Complex **8** could catalyze the model reaction too, with a short induction period. The rate of the reaction catalyzed by **8** at 25 °C was slower than that with **1**. The kinetic behavior of this complex is not discussed here because PPh_3 (1 equiv relative to Pd) in the system would compete for the coordination site on the Pd center during the whole catalytic process and would make the kinetic analysis more complicated.
[59] MeZnCl was used for simplicity of the NMR spectra.
[60] H.-B. Kraatz, M. E. van der Boom, Y. Ben-David, D. Milstein, *Isr. J. Chem.* **2001**, *41*, 163–171.
[61] CCDC-721678 (**2**), 721679 (**8**), and 721680 (**10**) contains the supplementary crystallographic data for this paper. These data can be obtained free of charge from The Cambridge Crystallographic Data Centre via www.ccdc.cam.ac.uk/data_request/cif.
[62] A third cycle was also possible, which consists of alkylation from **III** to **IV**, an alkyl shift from the Pd^{II} species to the S anion to result in the Pd^0 species, oxidative addition of the aryl iodide to the Pd^0 species, and an alkyl shift from the S anion to the Pd^{II} species to release the product and **III**. See Scheme 1 in the Supporting Information.
[63] The catalytic cycle might be a Pd^{II}–Pd^{IV} catalytic cycle, although there is not enough data to support the Pd^{IV} oxidation state.
[64] A. E. Jensen, W. Dohle, P. Knochel, *Tetrahedron* **2000**, *56*, 4197–4201.
[65] iC IR, version 1.05, Reaction Analysis Software for Chemical Development, AutoChem, Mettler-Toledo (USA).
[66] SMART, version 5.625, Area Detector Software Package and SAX Area Detector Integration Program, Brucker Analytical, Madison, WI (USA), **1997**.
[67] SAINT, version 6.45, Area Detector Software Package and SAX Area Detector Integration Program, Brucker Analytical, Madison, WI (USA), **1997**.
[68] SADABS, version 2.03, Area Detector Software Package and SAX Area Detector Integration Program, Brucker Analytical, Madison, WI (USA), **1997**.
[69] G. M. Sheldrick, SHELXTL, version 6.14, Crystal Structure Analysis Package, Brucker Analytical, Madison WI (USA), **1997**.
[70] F. Macaev, G. Rusu, S. Pogrebnoi, A. Gudima, E. Stingaci, L. Vlad, N. Shvets, F. Kandemirli, A. Dimoglo, R. Reynolds, *Bioorg. Med. Chem.* **2005**, *13*, 4842–4850.

Received: October 28, 2008
Revised: January 14, 2009
Published online: March 13, 2009

